

All-microwave holonomic control of an electron-nuclear two-qubit register in diamond

V. O. Shkolnikov and Guido Burkard

Department of Physics, University of Konstanz, D-78457 Konstanz, Germany

We present a theoretical scheme that allows to perform a universal set of holonomic gates on a two qubit register, formed by a ^{13}C nuclear spin coupled to the electron spin of a nitrogen-vacancy center in diamond. Strong hyperfine interaction between the electron spin and the spins of the first three shells of ^{13}C atoms allows to operate the state of the register on the submicrosecond timescale using microwave pulses only. We describe the system and the operating regime analytically and numerically, as well as simulate the initialization protocols.

I. INTRODUCTION

The negatively charged nitrogen vacancy (NV^-) center in diamond is a point defect, that has attracted significant attention in the recent years. Its bright optical transition with the zero phonon line of 1.945 eV [1, 2] and the existence of intersystem crossing provides a good mechanism for initialization and read out of a defect's spin state [3]. The ground state of the NV^- center is a spin triplet and is sensitive to magnetic and electric fields, as well as to strain [4–6], which makes the defect useful for metrological applications [7–9]. The long lifetime of the ground state coherence [10] together with the fast optical initialization and readout renders the NV center interesting for quantum information purposes [11, 12]. Recently fault tolerant universal geometric single-qubit gates [13] have been achieved both using optical [14, 15] and microwave [16, 17] control of the spin. Scaling up to many NV spins is still an issue, as it is challenging to couple the defect spins [18–20]. On the other hand, numerous experiments have been performed on multiqubit registers that include the NV center electron spin coupled to the nearby ^{13}C nuclear spins through the hyperfine interaction [21–26]. Such a configuration allows the use of the longer coherence time of the nuclear spin to preserve the quantum state during times exceeding the T_2^* of the electron spin. This can then be used for distributed quantum computation with electron-nuclear quantum registers [27] or to gain increased sensitivity in metrological applications of NV centers [28]. From this perspective the feasibility of universal control of the state of such registers becomes important. The existing experiments described in the literature [29] allow fast microwave control of the electron spin, as well as fast entangling CNOT or CPHASE gates controlled with the state of the nuclear spin. At the same time performing single qubit gates on the nuclear spins that are relatively close to the electron spin still required radio frequency pulses, that weakly couple to the nuclear spins due to their low gyromagnetic ratio [30].

Our work is motivated by the fact that the hyperfine interaction between the nearest neighbour ^{13}C nuclear spin and an NV center provides a nuclear spin splitting of the order of 130 MHz [31, 32], which allows for universal holonomic [13] single and two-qubit gates on the two-qubit register, assisted by hyperfine interaction. The

key enabling idea is to use a magnetic field to mix the electronic states $| -1 \rangle$ and $| 0 \rangle$. In this case the quantization axis for the nuclear spin will depend on the state of the electron spin. We will show that this implies that electronic transitions between different hyperfine levels are no longer forbidden by nuclear spin selection rules and can efficiently be driven by microwaves. This should result in a speed-up compared to the existing schemes and provide universal control of the register, requiring application of microwave-only pulses and making use of the relatively stronger electron magnetic dipolar transitions.

This paper is structured as follows. In section II we will consider our scheme in the leading order of perturbation theory, providing a more detailed treatment in the Appendix A. In section III we will discuss how one could initialize and read out the state of the two-qubit register. Section IV will be concerned with the construction of the pulses for universal quantum computing on the two-qubit system.

II. SYSTEM AND OPERATING REGIME

The Hamiltonian describing the ground state of the NV interacting with the nuclear spin of a nearby ^{13}C is

$$\begin{aligned}\hat{H}_{gs} &= \hat{H}_e + \hat{H}_n + \hat{H}_{hf}, \\ \hat{H}_e &= D_{gs} \hat{S}_z^2 + \gamma_e \mathbf{B} \cdot \hat{\mathbf{S}}, \\ \hat{H}_n &= \gamma_n \mathbf{B} \cdot \hat{\mathbf{I}}, \\ \hat{H}_{hf} &= \sum_{i,j=\{x,y,z\}} A_{ij} \hat{S}_i \hat{I}_j.\end{aligned}\tag{1}$$

Here $D_{gs} = 2.88$ GHz is the ground state zero-field splitting, $\gamma_e = g\mu_B = 2.8$ MHz/G is the electronic gyromagnetic ratio and $\gamma_n = 0.001$ MHz/G is the nuclear gyromagnetic ratio. The values for the hyperfine tensor A_{ij} are taken from [31]. This tensor is approximately diagonal in the basis, where the z-axis coincides with the direction connecting the vacancy to the ^{13}C atom. The eigenvalue corresponding to this axis amounts to 201 MHz for a ^{13}C atom in the first coordination shell, while the other two eigenvalues are 120 MHz. In our simulations we do a basis change to obtain the values of the tensor in the NV-axial basis. In what follows we will neglect the splittings arising due to the Zeeman Hamiltonian \hat{H}_n , as they

are much smaller than those arising from hyperfine interaction for the ^{13}C atom in the first coordination shell of an NV center.

Let us first treat the electronic part of the Hamiltonian (1), later we will add the hyperfine interaction as a perturbation. We first assume magnetic field $B_z = D_{gs}/\gamma_e$ in the direction of the NV symmetry axis, so that the levels $|-1\rangle$ and $|0\rangle$ are degenerate. Now we also assume a magnetic field B_\perp in the direction perpendicular to the symmetry axis, and write the magnetic field as $B_x - iB_y = B_\perp e^{i\phi}$. The coupling of $|1\rangle$ to $|0\rangle$ is suppressed due to a large energy gap $2D_{gs}$ between them, therefore, in this section we neglect this coupling. Thus the eigenvectors of the Hamiltonian will be $|+\rangle = (e^{i\phi/2}|0\rangle + e^{-i\phi/2}|-1\rangle)/\sqrt{2}$ and $|-\rangle = (e^{i\phi/2}|0\rangle - e^{-i\phi/2}|-1\rangle)/\sqrt{2}$ with the energies $\pm|\Omega|$ respectively, with $|\Omega| = \gamma_e B_\perp/\sqrt{2}$. Now we add the hyperfine interaction \hat{H}_{hf} to the system. Assuming $\|A\| \ll |\Omega|$, we can restrict our analysis to the secular terms of the hyperfine interaction, that do not flip the electron spin. Then for each electronic level we can describe the hyperfine interaction in terms of the Knight field h_j , acting on the nuclear spin I_j ,

$$\begin{aligned} \hat{H}_{hf} &= \sum_{e=\{+,-,1\}} \sum_{j=\{x,y,z\}} |e\rangle \langle e| h_j^e \hat{I}_j, \\ h_j^e &= \sum_{i=\{x,y,z\}} A_{ij} \langle e | \hat{S}_i | e \rangle. \end{aligned} \quad (2)$$

One of the key ingredients of the current proposal is the fact that the Knight field turns out to point in different directions for each of the three electronic levels, resulting in the level structure of the defect's ground state shown in Fig. 1. We can thus conclude that transitions between all eigenlevels of the system are now allowed by the nuclear spin selection rules and can be driven with a microwave field, oriented in the direction perpendicular to the symmetry axis of the defect. Let us number the levels in the figure from bottom to the top with 1, ..., 6. For a given direction of the microwave field, resonant with the transition from level i to level j , the Hamiltonian of the microwave field takes the form

$$\hat{H}_{mw} = g_{ij} (s_{ij} e^{i\omega_{ij}t} |i\rangle \langle j| + h.c.). \quad (3)$$

Here $\omega_{ij} = E_i - E_j$ is the energy splitting between levels i and j , s_{ij} is the matrix element, describing the strength of the corresponding microwave transition, g_{ij} is the amplitude of the microwave pulse, proportional to the magnetic field amplitude. In the simple picture described above, that neglects all nonsecular terms, one calculates w_{ij} as the difference between eigenvalues of the Hamilto-

nian (1), that includes only the secular terms

$$\begin{aligned} \hat{H} &= \left(-|\Omega| + \sum_{j=\{x,y,z\}} h_j^- \hat{I}_j \right) |- \rangle \langle -|, \\ &+ \left(|\Omega| + \sum_{j=\{x,y,z\}} h_j^+ \hat{I}_j \right) | + \rangle \langle +|, \\ &+ \left(2D_{gs} + \sum_{j=\{x,y,z\}} h_j^1 \hat{I}_j \right) |1\rangle \langle 1|. \end{aligned} \quad (4)$$

To parametrize h_j^e , $e \in \{+, -, 1\}$, we introduce $\theta^\pm, \phi^\pm, \theta^1, \phi^1$ according to

$$\begin{aligned} \mathbf{h}^e &= (h_x^e, h_y^e, h_z^e) \\ &= |h^e| (\sin \theta^e \cos \phi^e, \sin \theta^e \sin \phi^e, \cos \theta^e), \end{aligned} \quad (5)$$

for $e \in \{+, -, 1\}$.

The eigenstates of the system in Fig. 1 will take the

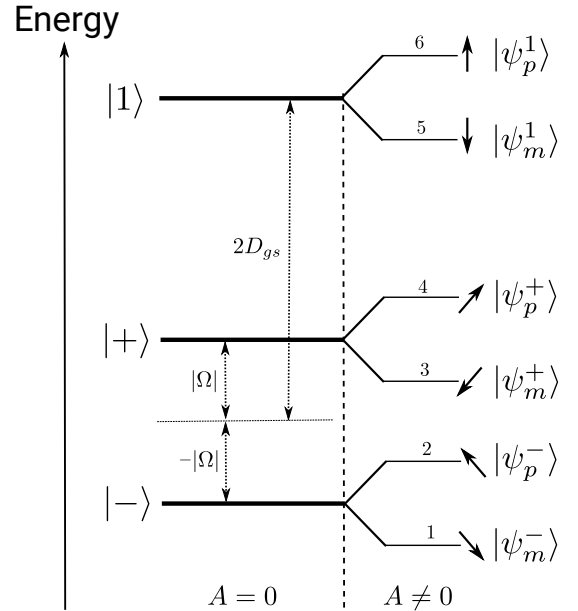


Figure 1. Energy level structure of the ground state of the NV⁻ center in diamond coupled to a nearby ^{13}C nuclear spin when a nonparallel magnetic field mixes the electronic levels $|0\rangle$ and $|-1\rangle$. The states $|+\rangle$, $|-\rangle$ and $|1\rangle$ to the left of the dashed line are the eigenstates of the electron spin without hyperfine interaction (hyperfine tensor $A = 0$), the direction of the black arrows to the right of the dashed line indicates the quantization axis of the nuclear spin and $|\psi_{p,m}^e\rangle$ ($e \in \{+, -, 1\}$) mark the corresponding hyperfine eigenstates. D_{gs} is the NV⁻ ground state zero field splitting, while $|\Omega|$ marks the splitting that arises between $|+\rangle$ and $|-\rangle$ when nonparallel magnetic field mixes $|0\rangle$ and $|-1\rangle$.

form

$$\begin{aligned}\psi_p^e &= |e\rangle \begin{pmatrix} \cos(\frac{\theta^e}{2}) \\ \sin(\frac{\theta^e}{2})e^{i\phi^e} \end{pmatrix}, \\ \psi_m^e &= |e\rangle \begin{pmatrix} \sin(\frac{\theta^e}{2}) \\ -\cos(\frac{\theta^e}{2})e^{i\phi^e} \end{pmatrix},\end{aligned}\quad (6)$$

with the eigenvalues being $E_{1,2} = -|\Omega| \pm |h^-|/2$, $E_{3,4} = |\Omega| \pm |h^+|/2$, $E_{5,6} = 2D_{gs} \pm |h^1|/2$. The state with index p corresponds to the upper state of the hyperfine doublet, with index m to the lower one. If the system is driven with a microwave field pointing in the y -direction, s_{ij} from equation (3) can be explicitly calculated using the states (6). For example s_{26} will take the form

$$\begin{aligned}s_{26} &= \langle \psi_p^- | S_y | \psi_p^1 \rangle \\ &= \langle - | S_y | 1 \rangle \left[\cos(\frac{\theta^-}{2}) \cos(\frac{\theta^1}{2}) + \sin(\frac{\theta^-}{2}) \sin(\frac{\theta^1}{2}) \right].\end{aligned}\quad (7)$$

The last factor here comes from the scalar product of two nuclear spin wave functions and its absolute value is $\cos(\alpha) = (\mathbf{h}^- \cdot \mathbf{h}^1) / (|\mathbf{h}^-| |\mathbf{h}^1|)$.

To gain universal control over the system we propose to use eight microwave pulses, that couple the levels 1, 2, 3, 4 to the levels 5, 6 (Fig. 1). The control Hamiltonian will then contain eight copies of (3) with $i \in \{5, 6\}$, $j \in \{1, 2, 3, 4\}$. If we change into a rotating frame, in which all the six levels have the same energy, the control Hamiltonian will take the form

$$\hat{H}_{\text{mw}} = \sum_{i \in \{5, 6\}, j \in \{1, 2, 3, 4\}} g_{ij} s_{ij} |i\rangle \langle j| + \text{h.c.} \quad (8)$$

Adjusting the two amplitudes g_{61} , g_{62} , we can couple any superposition of levels $|1\rangle$, $|2\rangle$ to the state $|6\rangle$. Let us now choose any pair of orthogonal nuclear spin states $|0_n\rangle$, $|1_n\rangle$, then

$$\begin{aligned}|-, 0_n\rangle &= \alpha |1\rangle + \beta |2\rangle, \\ |-, 1_n\rangle &= -\beta^* |1\rangle + \alpha^* |2\rangle.\end{aligned}\quad (9)$$

If we now apply the two pulses simultaneously, one coupling the level 1 to the level 6 and one coupling the level 2 to 6, such that $g_{61} = g\alpha^*/s_{61}$, $g_{62} = g\beta^*/s_{62}$, the control Hamiltonian will take the form $\hat{H}_{\text{mw}} = g|6\rangle \langle -, 0_n| + \text{h.c.}$. Analogously, if we define $g_{61} = -g\beta/s_{61}$, $g_{62} = g\alpha/s_{62}$, we will obtain the control Hamiltonian $\hat{H}_{\text{mw}} = g|6\rangle \langle -, 1_n| + \text{h.c.}$. These pairs of pulses are the new control pulse protocols that can couple $|-, 0_n\rangle$ and $|-, 1_n\rangle$ to the level $|6\rangle$. Similarly, we can define in total eight new control pulse protocols that will couple the levels $|-, 0_n\rangle$, $|-, 1_n\rangle$, $|+, 0_n\rangle$, $|+, 1_n\rangle$ to the levels $|5\rangle$ and $|6\rangle$. We name these new pulse protocols p_1, p_2, \dots, p_8 and show them in the Fig. 2. Each of these pulses has a magnitude $|p_i|$ and a phase f_i . In the rotating frame all states have the same energy, but in a real system the possibility to apply each of the given pulse protocols separately is based on the fact that the energy differences between levels 1, 2, 3, 4 and the levels 5, 6 in

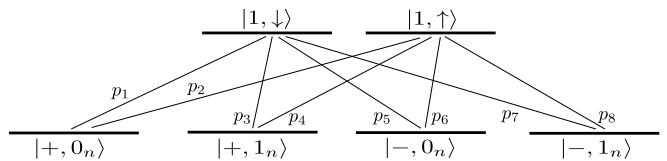


Figure 2. Eight different pulse protocols to couple any basis state of a two-qubit register to the upper electronic state of the NV center.

Fig. 1 have eight different values and the corresponding transitions can be resolved. In Fig. 1 the transition from level 1 to level 5 and from level 2 to level 6 are closest to each other. Choosing the parameters as discussed in Appendix B, we numerically diagonalize the Hamiltonian (1) and find that the closest resonance frequencies differ by 36 MHz, which suffices to resolve them.

In this section we based our description on the simplified Hamiltonian (4), that neglects the nonsecular interaction of the electron spin with nonparallel magnetic field and nonsecular hyperfine interaction terms. The same arguments can be given if one uses a more rigorous effective Hamiltonian (A10), that we derive in the Appendix A. This Hamiltonian takes into account the nonsecular interaction terms and is valid to second order perturbation theory.

III. INITIALIZATION AND READOUT

In this section we show how to perform initialization and readout of the system in the regime, suggested in the previous section, when $B_z = D_{gs}/\gamma_e$ and $|\Omega| \gg \|A\|$. Our proposal to perform initialization and readout of the system is based on coherent population trapping (CPT) [33] and resembles the scheme used in Ref. [34]. Figure 3 shows the procedure. Here the excited state manifold consists of an orbital doublet, spin triplet and a hyperfine doublet, thus forming a twelve-dimensional space. The exact Hamiltonian, governing the dynamics of the excited state manifold will be given in the Appendix B. The electronic levels $|1\rangle$, $|+\rangle$ are coupled to the excited state manifold through optical excitation, shown as red arrows in the Fig. 3. The frequencies of the optical fields are such that the level $|-\rangle$ is out of resonance, while the other two levels $|1\rangle$, $|+\rangle$ are coupled close to resonance. In Appendix B we show that one can achieve this with a single frequency optical field in the relevant magnetic field regime. In order to initialize the system in the lowest level of Fig. 3, an additional microwave pulse is required, shown as a blue arrow in Fig. 3. Whenever the lowest level is not populated, it will be brought to the excited state manifold through a combination of microwave and optical pulses. From there, the population will incoherently decay back to the ground state manifold through the channels marked with green arrows in the Fig. 3. Then the process repeats itself until after many cycles of optical and microwave excitation the population becomes

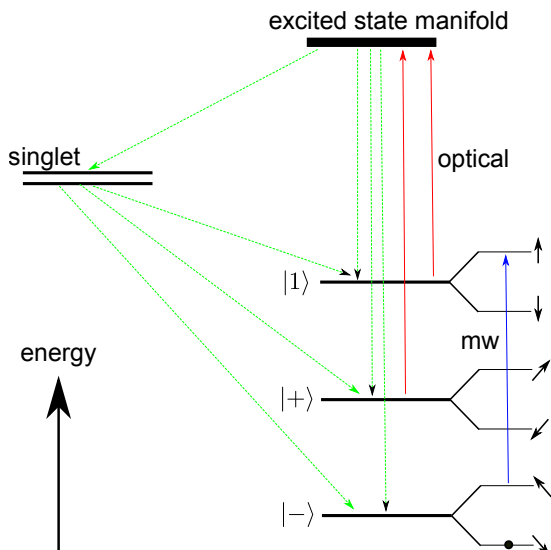


Figure 3. State initialization protocols. Optical pulses (red) pump the electronic states $|1\rangle$ and $|+\rangle$ to the NV excited state manifold. An additional simultaneous microwave tone (blue arrow) pumps one of the two lowest hyperfine sublevels. Green arrows illustrate incoherent mechanisms that return the population to the ground state. After many excitation cycles the system becomes trapped in the lower hyperfine level (black dot).

trapped in the lowest level of Fig. 3. We performed a numerical simulation of this initialization procedure and showed that in $100 \mu\text{s}$ the system can be initialized with a fidelity of 98%, in agreement with the results obtained for a similar procedure in [34]. The details of the simulation and the relevant parameters are given in Appendix B.

Read out can be performed in a similar manner. Let us assume that we want to know whether the system is in a state ψ . We first perform a gate that takes ψ to the lowest level of Fig. 3, followed by the initialization procedure. The absence of luminescence intensity indicates the system was initially in the state ψ , the presence of luminescence intensity indicates the opposite measurement result.

IV. UNIVERSAL SET OF HOLONOMIC GATES

We now show how to construct a universal set of gates to control the two-qubit register in the magnetic field regime given in section II, when $B_z = D_{gs}/\gamma_e$ and $|\Omega| \gg |A|$. Universal control requires that one can perform each of the eight microwave tones p_1, p_2, \dots, p_8 , without driving any other transitions. Our proposal is to perform nonabelian holonomic gates [13] using the setup described in the previous sections. Each step of such a gate requires the identification of a Λ -system, built from two lower and one upper state from Fig. 2. The lower states are coupled to the excited state with two different

lasers, that are both detuned from resonance by the same value Δ , as shown in Fig. 4.

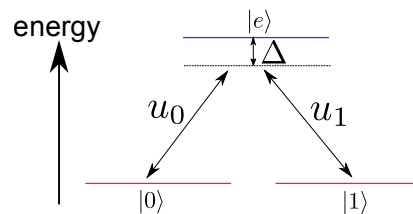


Figure 4. Energy levels in Λ -configuration. Two different lasers with amplitudes u_0 and u_1 and a common detuning Δ couple the ground states $|0\rangle$ and $|1\rangle$ to the same excited state $|e\rangle$. This generates nontrivial unitary operation on the lower levels, when the system is driven to the $|e\rangle$ state and back.

The Λ -system Hamiltonian reads

$$\hat{H}_\lambda = \sum_{k=1}^2 \left(u_k |k\rangle \langle e| + u_k^* |e\rangle \langle k| \right) + \Delta |e\rangle \langle e| \quad (10)$$

and as shown in [13], can be used to perform universal set of gates on the levels $|0\rangle$ and $|1\rangle$, if one can control the complex amplitudes u_1 and u_0 and the detuning Δ and the lasers are switched on for the duration $\tau = 2\pi/\sqrt{\Delta^2 + 4|u_0|^2 + 4|u_1|^2}$.

Figure 2 suggests different ways to identify such a Λ -system. Using the pulses p_1 and p_3 we can create a Λ -system that allows one to perform universal gates on the nuclear spin controlled by the state of an electron spin. More precisely, the nuclear spin state is flipped only if the electron spin is in the state $|+\rangle$. Analogously, using the pulses p_5 and p_7 one arrives at gates on the nuclear spin, controlled with the $|-\rangle$ state of the electron spin. Performing the same gate first using the pulses p_1 and p_3 and then the pulses p_5 and p_7 , one performs universal single qubit gates on the nuclear spin. In exactly the same way, gates on the electron spin controlled with the state of a nuclear spin can be performed combining pulses p_1 with p_5 and p_3 with p_7 . Thus, universal holonomic computation with the two-qubit register can be achieved.

For example, the CPHASE gate can be performed if the control pulse protocol p_8 is switched on with zero detuning for the time $\tau = \pi/|p_8|$. That is equivalent to switching two laser pulses that resonantly couple the levels 1 and 2 to the level 6 (Fig. 1). The amplitudes and phases of the lasers are adjusted such that the microwave Hamiltonian takes the form

$$\begin{aligned} \hat{H}_{\text{mw}} &= |6\rangle (g_{61}s_{61} \langle 1| + g_{62}s_{62} \langle 2|) + \text{h.c.} \\ &= p_8 |6\rangle \langle -, 1_n| + \text{h.c.} \end{aligned} \quad (11)$$

V. DISCUSSION

In this work we have shown how to perform universal quantum computing on a two qubit register, consisting

of the electron spin of a negatively charged nitrogen-vacancy center in diamond and the nuclear spin of a nearby ^{13}C atom. Although we only considered the carbon atom of the shell closest to the vacancy due to the strong hyperfine interaction, our method can be extended to control the carbon atoms further away. We estimate that the magnitude of the dipole-dipole hyperfine interaction for ^{13}C atoms that are twice as far from the vacancy as the closest carbon is such that the transitions $|1\rangle$ to $|5\rangle$ and $|2\rangle$ to $|6\rangle$ can still differ by 1 MHz and thus the register can be manipulated using microwave transitions only. The density functional theory calculations [35] that also take into account the Fermi contact term reveal there are approximately 40 carbon atoms around the vacancy with hyperfine constants greater than 2 MHz, which suggests that there are more than 3 closest ^{13}C atoms, to which our method can be applied. It is still possible to perform universal gates on these atoms until the electron spin decoheres, but in that case one also has to include the nitrogen nuclear spin into consideration. Our method can readily be extended to include the nitrogen nuclear spin through the hyperfine interaction Hamiltonian

$$\hat{H}_N = A_{\parallel} \hat{S}_z \hat{I}_z + A_{\perp} (\hat{S}_x \hat{I}_x + \hat{S}_y \hat{I}_y), \quad (12)$$

with the hyperfine constants being $A_{\parallel} = -2.16$ MHz, $A_{\perp} = -2.6$ MHz [36]. Using this Hamiltonian, the Knight field acting on the nitrogen nuclear spin can be calculated in the same way as it was done for the closest shell carbon atom. Other proposals exist to perform universal microwave control on the registers of coupled nuclear and electron spins [37, 38]. They differ from our method in the sense that their gates are not geometric and universality in those schemes requires an external magnetic field acting on the nuclear spins to add up with the hyperfine Knight field and thus create two nonparallel axes of rotation, while in our scheme we only rely on the hyperfine field, that is stronger than the external magnetic field. Strong hyperfine interaction has its disadvantages in that it decoheres the nuclear spin very fast. Going to a rotating frame picture reveals that the nuclear spin is not affected by the dephasing in the ground state space of the electron spin (T_2), but the relaxation processes (T_1), as well as reinitialization of the electron spin affect the nuclear spin dramatically [22]. Still our scheme can be used to perform universal quantum computation, for example, to gain increased sensitivity of an NV based quantum sensor [28]. We also note that although we only considered our scheme applied to the nuclear spin strongly coupled to the electronic spin, it would also be possible to consider it with respect to weakly coupled nuclear spins. A lot of research is done on the control of these registers [39–42] and configuration, in which the levels $|0\rangle$ and $|-1\rangle$ are mixed due to nonparallel magnetic field could offer new pathways to control such registers.

Appendix A: Effective Hamiltonian for hyperfine interaction in each electronic level, valid to second order perturbation theory

In this appendix we treat the coupled nuclear and electron spin system in the presence of nonparallel magnetic field in a rigorous way. We fix $B_z = D_{gs}/\gamma_e$ and introduce the phase factor ϕ according to the equation $B_x - iB_y = B_\perp e^{i\phi}$. At this field and in this notation one obtains

$$\begin{aligned}\hat{H}_e &= D_{gs}\hat{S}_z^2 + \gamma_e \left(B_x\hat{S}_x + B_y\hat{S}_y + B_z\hat{S}_z \right) \\ &= 2D_{gs}|1\rangle\langle 1| + \frac{\gamma_e}{2}B_\perp \left(e^{i\phi}S_+ + e^{-i\phi}S_- \right).\end{aligned}\quad (\text{A1})$$

We further introduce $\Omega = \frac{e^{3i\phi/2}}{2}\gamma_e B_\perp$ and the new basis states

$$\begin{aligned}|+\rangle &= \frac{1}{\sqrt{2}} \left(e^{i\phi/2}|0\rangle + e^{-i\phi/2}| -1\rangle \right), \\ |-\rangle &= \frac{1}{\sqrt{2}} \left(e^{i\phi/2}|0\rangle - e^{-i\phi/2}| -1\rangle \right),\end{aligned}\quad (\text{A2})$$

so the Hamiltonian H_e takes the form

$$\begin{aligned}\hat{H}_e &= \hat{H}^0 + \hat{H}_e^2, \\ \hat{H}^0 &= 2D_{gs}|1\rangle\langle 1| + |\Omega|(|+\rangle\langle +| - |-\rangle\langle -|), \\ \hat{H}_e^2 &= \Omega(|1\rangle\langle +| + |1\rangle\langle -|) + \Omega^*(|+\rangle\langle 1| + |-\rangle\langle 1|).\end{aligned}\quad (\text{A3})$$

We now introduce the hyperfine and the nuclear spin Zeeman interactions \hat{H}_{hf} , \hat{H}_n into the system. We split the hyperfine interaction into secular and nonsecular terms as

$$\begin{aligned}\hat{H}_{hf} &= \hat{H}_{hf}^1 + \hat{H}_{hf}^2 \\ \hat{H}_{hf}^1 &= \sum_{k=\{1,+,-\}} |k\rangle\langle k| \sum_{i,j=\{x,y,z\}} A_{ij}\hat{I}_j \langle k|\hat{S}_i|k\rangle, \\ \hat{H}_{hf}^2 &= \sum_{\tilde{k}\neq k} |k\rangle\langle \tilde{k}| \sum_{i,j=\{x,y,z\}} A_{ij}\hat{I}_j \langle k|\hat{S}_i|\tilde{k}\rangle.\end{aligned}\quad (\text{A4})$$

Our aim now is to obtain an effective Hamiltonian in each of the three electronic subspaces. We achieve this using the formalism of the Schrieffer-Wolf transformation [43, 44]. The basic idea is to find a basis change that brings to zero non-secular terms \hat{H}_e , \hat{H}_{hf}^2 up to a certain order of magnitude. In order for this procedure to work we have to assume that $|\Omega| \ll 2D_{gs}$, $\|A_{ij}\| \ll 2\Omega$. Following this procedure, we introduce an antihermitian matrix S , that obeys the equation

$$SH_e^0 - H_e^0S = -\hat{H}_{hf}^2 - \hat{H}_e^2. \quad (\text{A5})$$

After performing this procedure, we obtain

$$\begin{aligned}S &= \frac{\Omega}{2D_{gs} - |\Omega|} |1\rangle\langle +| + h.c. \\ &+ \frac{\Omega}{2D_{gs} + |\Omega|} |1\rangle\langle -| + h.c. \\ &- \sum_{k\neq\tilde{k}} \frac{\sum_{ij} A_{ij}\hat{I}_j \langle k|\hat{S}_i|\tilde{k}\rangle}{W_{\tilde{k}} - W_k},\end{aligned}\quad (\text{A6})$$

where W_1 , W_+ and W_- are $2D_{gs}$, $|\Omega|$ and $-|\Omega|$ respectively. Now we can calculate the effective Hamiltonian in each of the three electronic subspaces

$$\hat{H}_{\text{eff}} = \hat{H}_e^0 + \hat{H}_n + \hat{H}_{hf}^1 + \frac{1}{2} \left[S, \hat{H}_{hf}^2 + \hat{H}_e^2 \right]. \quad (\text{A7})$$

From this expression it follows that the interaction of the electron spin with the transverse magnetic field leads to the renormalization of the energies of the bare electronic states D_{gs} , $|\Omega|$, $-|\Omega|$ to the new values

$$\begin{aligned}\tilde{D}_{gs} &= D_{gs} \left(1 + \frac{2|\Omega|^2}{4D_{gs}^2 - |\Omega|^2} \right) \\ \Omega_\pm &= |\Omega| \left(1 \mp \frac{|\Omega|}{2D_{gs} \mp |\Omega|} \right)\end{aligned}\quad (\text{A8})$$

Let us also introduce the corrections to hyperfine terms due to the interaction of electron spin with the transverse magnetic field

$$C_\pm = \frac{2\text{Re}[\Omega \langle \pm | \hat{S}_i | 1 \rangle]}{2D_{gs} \mp |\Omega|} \quad (\text{A9})$$

For the effective Hamiltonian we then obtain

$$\begin{aligned}\hat{H}_{\text{eff}} &= 2\tilde{D}_{gs}|1\rangle\langle 1| + \Omega_+|+\rangle\langle +| - \Omega_-|-\rangle\langle -| \\ &+ \sum_{ij} A_{ij}\hat{I}_j \left(\langle 1|\hat{S}_i|1\rangle + C_+ + C_- \right) |1\rangle\langle 1| \\ &+ \sum_{ij} A_{ij}\hat{I}_j \left(\langle +|\hat{S}_i|+\rangle - C_+ \right) |+\rangle\langle +| \\ &+ \sum_{ij} A_{ij}\hat{I}_j \left(\langle -|\hat{S}_i|-\rangle - C_- \right) |-\rangle\langle -| \\ &+ \frac{1}{2} \sum_{ij} \frac{A_{ij}A_{i\tilde{j}}}{2|\Omega|} \langle +|\hat{S}_i|-\rangle \langle -|\hat{S}_{\tilde{i}}|+\rangle \hat{I}_j\hat{I}_{\tilde{j}} |+\rangle\langle +| \\ &- \frac{1}{2} \sum_{ij} \frac{A_{ij}A_{i\tilde{j}}}{2|\Omega|} \langle -|\hat{S}_i|+\rangle \langle +|\hat{S}_{\tilde{i}}|-\rangle \hat{I}_j\hat{I}_{\tilde{j}} |-\rangle\langle -| \\ &+ \hat{H}_n.\end{aligned}\quad (\text{A10})$$

The first line here arises due to the interaction of the electron spin with magnetic field. Lines two to four describe the secular terms of the hyperfine interaction corrected due to nonsecular terms of the electron spin interaction with the magnetic field. Lines five and six take into account nonsecular part of the hyperfine interaction, that mixes the electron spin states $|+\rangle$, $|-\rangle$. We neglect the effect of this interactions that mixes $|+\rangle$, $|-\rangle$ with $|1\rangle$, because it is small compared to all other effects.

Appendix B: Details of the dynamics simulation

In this appendix we give details of the simulation we performed to model the initialization fidelity. The ground state of the NV is an orbital singlet, spin triplet and we describe it with the Hamiltonian (1). The excited state is treated as an orbital doublet, spin triplet and we describe it with the following Hamiltonian [2]

$$\begin{aligned}
\hat{H}_{es} = & g_{es}^{\parallel} \mu_B B_z \hat{S}_z + 2\mu_B (B_x \hat{S}_x + B_y \hat{S}_y) \\
& - \lambda \sigma_y \hat{S}_z + l \mu_B B_z \sigma_y \\
& + D_{zz} \left(\hat{S}_z^2 - \frac{1}{3} S(S+1) \right) \\
& + D_{xy} \left(\sigma_z (\hat{S}_y^2 - \hat{S}_x^2) - \sigma_x \{ \hat{S}_x, \hat{S}_y \} \right) \\
& + D_{xz} \left(\sigma_z \{ \hat{S}_x, \hat{S}_z \} - \sigma_x \{ \hat{S}_y, \hat{S}_z \} \right) \\
& + \sum_{i,j=\{x,y,z\}} A_{ij}^{es} \hat{S}_i \hat{I}_j \\
& + \gamma_n \mathbf{B} \cdot \hat{\mathbf{I}}
\end{aligned} \tag{B1}$$

Here $\sigma_x, \sigma_y, \sigma_z$ are Pauli matrices that act in the basis of $|E_x\rangle, |E_y\rangle$ of the orbital doublet. The first line describes the Zeeman interaction, the second line takes into account spin-orbit coupling and the interaction of magnetic field with the orbital angular momentum \hat{L} (described with an operator σ_y in the relevant subspace). Lines three, four and five describe the spin-spin interaction. The sixth line takes into account the hyperfine interaction in the excited state. The seventh line gives the Zeeman interaction for the nuclear spin. The strength of the corresponding interactions is taken from Ref. [45] and is listed in Table I. The strength of the hyperfine interaction is given in the basis when z-axis coincides with the direction from the vacancy to the ^{13}C atom. In this basis the hyperfine tensor is diagonal, with the biggest eigenvalue (A_{\parallel}^{es}) corresponding to the vector along z-direction. The excited orbital states can decay to the ground state through a spin-conserving photon emission with the rate Γ_{ge} each. The corresponding decay operators are $O_x = |A_2\rangle \langle E_x|$ and $O_y = |A_2\rangle \langle E_y|$, where $|A_2\rangle$ is the ground state orbital singlet. The excited state $|A_1\rangle$, that is the eigenstate of the spin-orbit and spin-spin part of the Hamiltonian (B1), can also decay to the singlet level $|s\rangle$ with the rate Γ_{se} . The corresponding decay operator is $O_3 = |s\rangle \langle A_1|$. The singlet state can decay to the ground through three channels, to the state with spin 0 at the rate Γ_{0s} and corresponding decay operator $O_4 = |A_2, m_s = 0\rangle \langle s|$ or to the states with spins ± 1 with the rate Γ_{pms} and corresponding decay operators $O_5 = |A_2, m_s = +1\rangle \langle s|$ and $O_6 = |A_2, m_s = -1\rangle \langle s|$. The values of the decay rates are taken from Ref. [45] and are listed in Table I. We assumed the z-component of the magnetic field to be D_{gs}/γ_e . The transverse magnetic field is assumed to point in the x-direction and have the value of 500 G. We show that at this magnetic field

one optical field is enough to couple the electronic levels $|+\rangle$ and $|1\rangle$ to the excited state $|E_x\rangle$ (Figure 3), while leaving $|-\rangle$ out of resonance. The microwave magnetic field pulse in Fig. 3 is assumed to point in the y-direction. The corresponding optical and microwave Rabi frequencies Ω_o and Ω_{mw} respectively are given in Table I. The optical and microwave driving Hamiltonians are given by

$$\begin{aligned}
\hat{H}_o &= \Omega_o (|E_x\rangle \langle A_2| e^{i\omega_1 t} + |A_2\rangle \langle E_x| e^{-i\omega_1 t}), \\
\hat{H}_{mw} &= \Omega_{mw} \hat{S}_y \sin(\omega_2 t).
\end{aligned} \tag{B2}$$

We solve the Lindblad equation

$$\begin{aligned}
\dot{\rho} = & -\frac{i}{\hbar} [\hat{H}_{gs} + \hat{H}_{es} + \hat{H}_o + \hat{H}_{mw}, \rho] \\
& + \sum_{i=1}^6 \Gamma_i \left(\hat{O}_i \rho \hat{O}_i^\dagger - \frac{1}{2} \hat{O}_i^\dagger \hat{O}_i \rho - \frac{1}{2} \rho \hat{O}_i^\dagger \hat{O}_i \right),
\end{aligned} \tag{B3}$$

assuming the duration of the optical and microwave pulses of 100 μs . Our simulation reveals that assuming the system to be initially in equal superposition of the six ground states, after such procedure the system will be trapped in the lowest ground state with the probability 97%.

Table I. The values used to simulate the initialization fidelity.

Parameter	Value
g-factor g_{es}^{\parallel}	2.15
spin-orbit constant λ	5.33 GHz
l	0.1
axial spin-spin constant D_{zz}	1.44 GHz
transverse spin-spin constant D_{xy}	1.54 GHz
transverse spin-spin constant D_{xz}	154 MHz
A_{\parallel}^{es}	126 MHz
A_{\perp}^{es}	56.7 MHz
γ_n	0.001 MHz/G
Γ_{ge}	83.3 MHz
Γ_{se}	400 MHz
Γ_{0s}	1.5 MHz
Γ_{pms}	0.58 MHz
Ω_o	25 MHz
Ω_{mw}	10 MHz

- [1] J. R. Maze, A. Gali, E. Togan, Y. Chu, A. Trifonov, E. Kaxiras, and M. D. Lukin, *New Journal of Physics* **13**, 025025 (2011).
- [2] M. W. Doherty, N. B. Manson, P. Delaney, F. Jelezko, J. Wrachtrup, and L. C. Hollenberg, *Physics Reports* **528**, 1 (2013).
- [3] F. Jelezko, T. Gaebel, I. Popa, A. Gruber, and J. Wrachtrup, *Phys. Rev. Lett.* **92**, 076401 (2004).
- [4] M. S. J. Barson, P. Peddibhotla, P. Ovarthaiyapong, K. Ganesan, R. L. Taylor, M. Gebert, Z. Mielens, B. Koslowski, D. A. Simpson, L. P. McGuinness, J. McCallum, S. Prawer, S. Onoda, T. Ohshima, A. C. Bleszynski Jayich, F. Jelezko, N. B. Manson, and M. W. Doherty, *Nano Letters* **17**, 1496 (2017).
- [5] M. W. Doherty, F. Dolde, H. Fedder, F. Jelezko, J. Wrachtrup, N. B. Manson, and L. C. L. Hollenberg, *Phys. Rev. B* **85**, 205203 (2012).
- [6] P. Udvarhelyi, V. O. Shkolnikov, A. Gali, G. Burkard, and A. Pályi, *Phys. Rev. B* **98**, 075201 (2018).
- [7] G. Balasubramanian, I. Y. Chan, R. Kolesov, M. Al-Hmoud, J. Tisler, C. Shin, C. Kim, A. Wojcik, P. R. Hemmer, A. Krueger, T. Hanke, A. Leitenstorfer, R. Bratschkitsch, F. Jelezko, and J. Wrachtrup, *Nature* **455**, 648 (2008).
- [8] J. R. Maze, P. L. Stanwix, J. S. Hodges, S. Hong, J. M. Taylor, P. Cappellaro, L. Jiang, M. V. G. Dutt, E. Togan, A. S. Zibrov, A. Yacoby, R. L. Walsworth, and M. D. Lukin, *Nature* **455**, 644 (2008).
- [9] A. Barfuss, J. Teissier, E. Neu, A. Nunnenkamp, and P. Maletinsky, *Nature Physics* **11**, 820 (2015).
- [10] N. Mizuochi, P. Neumann, F. Rempp, J. Beck, V. Jacques, P. Siyushev, K. Nakamura, D. J. Twitchen, H. Watanabe, S. Yamasaki, F. Jelezko, and J. Wrachtrup, *Phys. Rev. B* **80**, 041201 (2009).
- [11] B. Hensen, H. Bernien, A. E. Dréau, A. Reiserer, N. Kalb, M. S. Blok, J. Ruitenber, R. F. L. Vermeulen, R. N. Schouten, C. Abellán, W. Amaya, V. Pruneri, M. W. Mitchell, M. Markham, D. J. Twitchen, D. Elkouss, S. Wehner, T. H. Taminiau, and R. Hanson, *Nature* **526**, 682 (2015).
- [12] E. Togan, Y. Chu, A. S. Trifonov, L. Jiang, J. Maze, L. Childress, M. V. G. Dutt, A. S. Sørensen, P. R. Hemmer, A. S. Zibrov, and M. D. Lukin, *Nature* **466**, 730 (2010).
- [13] E. Sjöqvist, *Physics Letters A* **380**, 65 (2016).
- [14] B. B. Zhou, P. C. Jerger, V. O. Shkolnikov, F. J. Heremans, G. Burkard, and D. D. Awschalom, *Phys. Rev. Lett.* **119**, 140503 (2017).
- [15] Y. Sekiguchi, N. Niikura, R. Kuroiwa, H. Kano, and H. Kosaka, *Nature Photonics* **11**, 309 (2017).
- [16] C. Zu, W.-B. Wang, L. He, W.-G. Zhang, C.-Y. Dai, F. Wang, and L.-M. Duan, *Nature* **514**, 72 (2014).
- [17] S. Arroyo-Camejo, A. Lazarev, S. W. Hell, and G. Balasubramanian, *Nature Communications* **5**, 4870 (2014).
- [18] F. Dolde, I. Jakobi, B. Naydenov, N. Zhao, S. Pezzagna, C. Trautmann, J. Meijer, P. Neumann, F. Jelezko, and J. Wrachtrup, *Nature Physics* **9**, 139 (2013).
- [19] W. Pfaff, T. H. Taminiau, L. Robledo, H. Bernien, M. Markham, D. J. Twitchen, and R. Hanson, *Nature Physics* **9**, 29 (2012).
- [20] G. Burkard, V. O. Shkolnikov, and D. D. Awschalom, *Phys. Rev. B* **95**, 205420 (2017).
- [21] L. Childress, M. V. Gurudev Dutt, J. M. Taylor, A. S. Zibrov, F. Jelezko, J. Wrachtrup, P. R. Hemmer, and M. D. Lukin, *Science* **314**, 281 (2006).
- [22] M. V. G. Dutt, L. Childress, L. Jiang, E. Togan, J. Maze, F. Jelezko, A. S. Zibrov, P. R. Hemmer, and M. D. Lukin, *Science* **316**, 1312 (2007).
- [23] P. Neumann, N. Mizuochi, F. Rempp, P. Hemmer, H. Watanabe, S. Yamasaki, V. Jacques, T. Gaebel, F. Jelezko, and J. Wrachtrup, *Science* **320**, 1326 (2008).
- [24] G. Waldherr, Y. Wang, S. Zaiser, M. Jamali, T. Schulte-Herbrüggen, H. Abe, T. Ohshima, J. Isoya, J. F. Du, P. Neumann, and J. Wrachtrup, *Nature* **506**, 204 (2014).
- [25] S. Yang, Y. Wang, D. D. B. Rao, T. Hien Tran, A. S. Momenzadeh, M. Markham, D. J. Twitchen, P. Wang, W. Yang, R. Stöhr, P. Neumann, H. Kosaka, and J. Wrachtrup, *Nature Photonics* **10**, 507 (2016).
- [26] P. C. Maurer, G. Kucsko, C. Latta, L. Jiang, N. Y. Yao, S. D. Bennett, F. Pastawski, D. Hunger, N. Chisholm, M. Markham, D. J. Twitchen, J. I. Cirac, and M. D. Lukin, *Science* **336**, 1283 (2012).
- [27] L. Jiang, J. M. Taylor, A. S. Sørensen, and M. D. Lukin, *Phys. Rev. A* **76**, 062323 (2007).
- [28] S. Zaiser, T. Rendler, I. Jakobi, T. Wolf, S.-Y. Lee, S. Wagner, V. Bergholm, T. Schulte-Herbrüggen, P. Neumann, and J. Wrachtrup, *Nature Communications* **7**, 12279 (2016).
- [29] F. Jelezko, T. Gaebel, I. Popa, M. Domhan, A. Gruber, and J. Wrachtrup, *Phys. Rev. Lett.* **93**, 130501 (2004).
- [30] P. Cappellaro, L. Jiang, J. S. Hodges, and M. D. Lukin, *Phys. Rev. Lett.* **102**, 210502 (2009).
- [31] A. Gali, *Phys. Rev. B* **80**, 241204 (2009).
- [32] S. Felton, A. M. Edmonds, M. E. Newton, P. M. Martineau, D. Fisher, D. J. Twitchen, and J. M. Baker, *Phys. Rev. B* **79**, 075203 (2009).
- [33] M. Fleischhauer, A. Imamoglu, and J. P. Marangos, *Rev. Mod. Phys.* **77**, 633 (2005).
- [34] L. Robledo, L. Childress, H. Bernien, B. Hensen, P. F. A. Alkemade, and R. Hanson, *Nature* **477**, 574 (2011).
- [35] A. Gali, M. Fyta, and E. Kaxiras, *Phys. Rev. B* **77**, 155206 (2008).
- [36] M. Chen, M. Hirose, and P. Cappellaro, *Phys. Rev. B* **92**, 020101 (2015).
- [37] J. S. Hodges, J. C. Yang, C. Ramanathan, and D. G. Cory, *Phys. Rev. A* **78**, 010303 (2008).
- [38] N. Khaneja, *Phys. Rev. A* **76**, 032326 (2007).
- [39] M. H. Abobeih, J. Randall, C. E. Bradley, H. P. Bartling, M. A. Bakker, M. J. Degen, M. Markham, D. J. Twitchen, and T. H. Taminiau, *arXiv:1905.02095 [quant-ph]* (2019).
- [40] T. H. Taminiau, J. J. T. Wagenaar, T. van der Sar, F. Jelezko, V. V. Dobrovitski, and R. Hanson, *Phys. Rev. Lett.* **109**, 137602 (2012).
- [41] S. B. van Dam, J. Cramer, T. H. Taminiau, and R. Hanson, *Phys. Rev. Lett.* **123**, 050401 (2019).
- [42] T. H. Taminiau, J. Cramer, T. van der Sar, V. V. Dobrovitski, and R. Hanson, *Nature Nanotechnology* **9**, 171 (2014).
- [43] R. Winkler, *"Spin-orbit coupling effects in two-dimensional electron and hole systems"*, Springer tracts in modern physics (Springer, Berlin, 2003).

- [44] S. Bravyi, D. P. DiVincenzo, and D. Loss, *Annals of Physics* **326**, 2793 (2011).
- [45] L. C. Bassett, F. J. Heremans, D. J. Christle, C. G. Yale, G. Burkard, B. B. Buckley, and D. D. Awschalom, *Science* **345**, 1333 (2014).